Development 134, 833-837 (2007) doi:10.1242/dev.02794

Morphogenesis defects are associated with abnormal nervous system regeneration following *roboA* RNAi in planarians

Francesc Cebrià* and Phillip A. Newmark†

The process by which the proper pattern is restored to newly formed tissues during metazoan regeneration remains an open question. Here, we provide evidence that the nervous system plays a role in regulating morphogenesis during anterior regeneration in the planarian *Schmidtea mediterranea*. RNA interference (RNAi) knockdown of a planarian ortholog of the axon-guidance receptor *roundabout* (*robo*) leads to unexpected phenotypes during anterior regeneration, including the development of a supernumerary pharynx (the feeding organ of the animal) and the production of ectopic, dorsal outgrowths with cephalic identity. We show that *Smed-roboA* RNAi knockdown disrupts nervous system structure during cephalic regeneration: the newly regenerated brain and ventral nerve cords do not re-establish proper connections. These neural defects precede, and are correlated with, the development of ectopic structures. We propose that, in the absence of proper connectivity between the cephalic ganglia and the ventral nerve cords, neurally derived signals promote the differentiation of pharyngeal and cephalic structures. Together with previous studies on regeneration in annelids and amphibians, these results suggest a conserved role of the nervous system in pattern formation during blastema-based regeneration.

KEY WORDS: Neural regeneration, Planarian, Axon guidance, ROBO, *Schmidtea mediterranea*

INTRODUCTION

Freshwater planarians possess amazing regenerative abilities: when cut transversely, the anterior-facing wound regenerates a new head, whereas the posterior-facing wound regenerates a new tail (Newmark and Sánchez Alvarado, 2002; Agata, 2003; Reddien and Sánchez Alvarado, 2004). After amputation, stem cells called neoblasts proliferate to produce the regeneration blastema in which the missing structures will regenerate (Newmark and Sánchez Alvarado, 2002; Reddien and Sánchez Alvarado, 2004). Previous studies suggest that differentiated cells convey the positional information required for proper morphogenesis in planarians (Saló and Baguñà, 1985; Kato et al., 2001) and that epithelial-mesenchymal interactions (Chandebois, 1980), as well as gap junctional communication (Nogi and Levin, 2005), may be important for defining anterior versus posterior regeneration. Recent large-scale RNA interference (RNAi) analysis identified hundreds of genes required for proper regeneration (Reddien et al., 2005); however, the exact mechanisms governing morphogenesis of the planarian regenerate are still largely unknown.

In the initial days of anterior regeneration, primordia of the cephalic ganglia form within the blastema; these cephalic ganglia must then re-establish proper connections with the ventral nerve cords and with each other (Cebrià et al., 2002; Cebrià and Newmark, 2005) to produce a functional central nervous system (CNS). To understand the mechanisms underlying the regeneration of the planarian CNS, we have begun to identify planarian orthologs of genes required for proper axon guidance (Cebrià and Newmark, 2005). Here, we report the isolation and functional characterization of a *roundabout* gene from the planarian *Schmidtea mediterranea* (*Smed-roboA*). ROBO proteins are evolutionarily conserved transmembrane receptors of the immunoglobulin superfamily that bind secreted molecules of the SLIT family (Brose et al., 1999; Kidd et al., 1999); together, they play important roles in guiding axons to their proper targets (Araujo and Tear, 2003; Inatani, 2005). RNAi knockdown of *Smed-roboA* results in the unexpected production of a supernumerary pharynx and ectopic cephalic outgrowth during anterior regeneration. We show that the development of these ectopic structures correlates with improper connectivity between the newly regenerated cephalic ganglia and the ventral nerve cords. These results suggest that the nervous system is a source of signal(s) required for proper morphogenesis during planarian regeneration.

MATERIALS AND METHODS

Organisms

A clonal line of the diploid, asexual strain of *Schmidtea mediterranea* was used (Sánchez Alvarado et al., 2002). Planarians were maintained as previously described (Cebrià and Newmark, 2005) and starved for at least 1 week before use.

Isolation of *Smed-robo* homologues

S. mediterranea genomic sequences encoding predicted proteins similar to ROBO were retrieved from the NCBI Trace Archives and assembled using Sequencher 4.2.2 (Gene Codes Corporation). In total, two different genes encoding predicted ROBO proteins were identified; both were amplified from a planarian cDNA library (Zayas et al., 2005) and RACE was used to obtain additional cDNA sequences. GenBank accession numbers for *Smed-roboA* and *Smed-roboB* are DQ336174 and DQ336175, respectively.

Whole-mount in situ hybridization and immunostaining

Planarians were processed in an Intavis InsituPro hybridization robot (Sánchez Alvarado et al., 2002) and imaged as described previously (Cebrià and Newmark, 2005). Immunostaining was performed as described (Cebrià

Department of Cell and Developmental Biology, Neuroscience Program, University of Illinois at Urbana-Champaign, B107 Chemical and Life Sciences Laboratory, 601 South Goodwin Avenue, Urbana, IL 61801, USA.

*Present address: Departament de Genètica, Universitat de Barcelona, Av. Diagonal 645, 08028 Barcelona, Spain
†Author for correspondence (e-mail: pnewmark@life.uiuc.edu)

Accepted 15 December 2006

and Newmark, 2005) using: anti-tubulin Ab-4 (NeoMarkers, 1:200) to label axon bundles of the ventral nerve cords (VNCs), transverse commissures and lateral processes; anti-phospho-tyrosine P-Tyr-100 (Cell Signaling Technology, 1:500) to visualize the brain, VNC ganglia, gut and pharynx; and VC-1 to label photosensitive cells (Umesono et al., 1999). Highly cross-absorbed Alexa Fluor 488 goat anti-mouse IgG secondary antibodies (Invitrogen) were used at 1:400. Samples were mounted in Vectashield (Vector Laboratories), imaged with a CARV spinning disc confocal microscope and deconvolved using AutoDeblur 9.3 (AutoQuant Imaging, Inc.).

RNAi analyses

Double-stranded RNA (dsRNA) was synthesized and injected as described previously (Sánchez Alvarado and Newmark, 1999; Cebrià and Newmark, 2005). Injected planarians were amputated pre-pharyngeally, allowed to regenerate and processed for in situ hybridization or immunostaining. At 15 days after the first round of injections, some regenerating animals were re-injected on 3 consecutive days and re-amputated. Control animals were injected with water or GFP dsRNA. No defects were observed in intact or regenerating animals after *Smed-roboB* RNAi knockdown. *Smed-roboA*; *Smed-roboB* double knockdowns showed the same phenotypes as *Smed-roboA* single knockdown; thus, we limit this report to *Smed-roboA*.

RESULTS AND DISCUSSION

Smed-roboA is required for the proper guidance of regenerating photoreceptor axons

We identified planarian robo homologues in genomic sequences from *S. mediterranea* (see Materials and methods). Similar to other robo-family members, *Smed-roboA* encodes five conserved immunoglobulin repeats and three fibronectin type III repeats in the extracellular domain (Fig. 1A). *Smed-roboA* mRNA is expressed in the CNS and pharyngeal nerve ganglia in intact planarians (Fig. 1B), as well as in the regenerating CNS (Fig. 1C-E) and pharynx (Fig. 1G).

To analyze the function of *Smed-roboA*, we performed RNAi (Sánchez Alvarado and Newmark, 1999). A reduction of endogenous transcript after *Smed-roboA* RNAi was confirmed by in situ hybridization (Fig. 1F,G,I,J). Specific inhibition was observed both within the newly regenerated tissues and within the pre-existing nervous system (Fig. 1I,J); the expression of *Smed-roboB* was unaffected (Fig. 1H,K). Conversely, *Smed-roboB* RNAi did not affect levels of the *Smed-roboA* transcript (data not shown). No abnormal phenotypes were observed in *Smed-roboA* knockdowns in intact animals (5 weeks after RNAi, two sets of three injections; n=10).

We monitored the effects of *Smed-roboA* RNAi on photoreceptor regeneration. Planarian photoreceptors consist of two cell types: pigment cup cells and photosensitive cells that reside outside of the pigment-cup opening. The photosensitive cells extend axons posteriorly in a stereotypical pattern; some axons project ipsilaterally, whereas others project contralaterally, forming an optic chiasm that extends to the brain (Okamoto et al., 2005) (Fig. 1L). *Smed-roboA* RNAi regenerates showed a variety of visual system defects (Fig. 1M-O): the most common phenotypes (39/47 vs 1/43 in controls; see Table S1 in the supplementary material) were ectopic projections that resulted in loops (Fig. 1M,N); in some specimens (8/47 vs 0/43 in controls), the visual axons projected to the most-

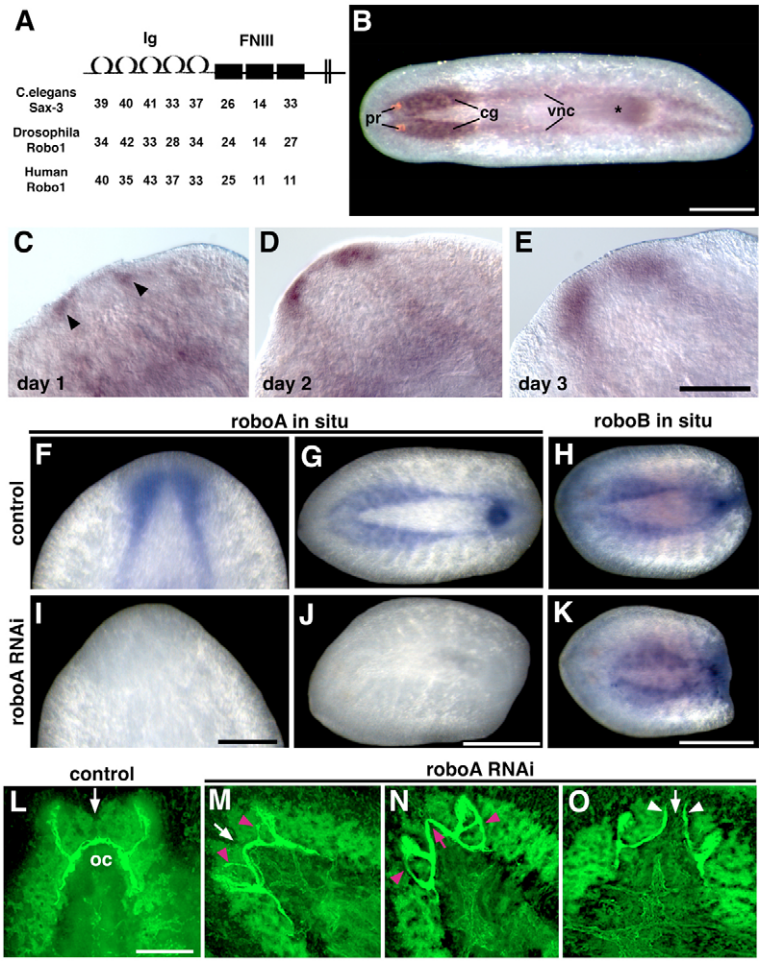

Fig. 1. Characterization of *Smed-roboA* and defects in visual-system regeneration after *Smed-roboA* RNAi. (**A**) Organization of the predicted SMED-ROBOA extracellular domain containing five immunoglobulin-like (Ig) and three fibronectin (FNIII) domains, compared to ROBO proteins from *C. elegans* (AF041053), *Drosophila* (AF040989) and human (AF040990). Numbers indicate percentage of identical amino acids in each domain. (**B-E**) *Smed-roboA* in situ hybridization in an intact planarian (B) and during anterior regeneration (C-E); days post-amputation are indicated. (C) Arrowheads show cephalic ganglia primordia. (**F-K**) Efficacy and specificity of *Smed-roboA* RNAi revealed by whole-mount in situ hybridization. (F-H) Control samples; (I-K) *Smed-roboA* samples. (F,G) Controls reveal normal expression of *Smed-roboA* during anterior and posterior regeneration, respectively. (I,J) After *Smed-roboA* RNAi, *roboA* transcript is not detected in newly regenerated or pre-existing tissues. (H,K) *Smed-roboA* RNAi does not affect *roboB* expression. (F,I) Trunk pieces at 6 days of anterior regeneration; (G,H,J,K) head pieces at 6 days of posterior regeneration. (**L-O**) Double immunofluorescence to label the cephalic ganglia (anti-phospho-tyrosine; pale green) and photosensitive cells (VC-1; bright green). (L) Control: photoreceptor axons project to the visual center in the brain, forming a normal optic chiasm (oc); arrow indicates normal anterior commissure. (M-O) *Smed-roboA* RNAi: ectopic projections appear (magenta arrowheads) and the shape of the chiasm is altered (magenta arrow in N). The anterior commissure is reduced (arrow in M) or absent (arrow in O). (L,M,O) After 16 days of regeneration. (N) After 35 days of regeneration. cg, cephalic ganglia; pr, photoreceptors; vnc, ventral nerve cords; asterisk, pharynx. Scale bars: 500 μm in B; 200 μm in C-E; 200 μm in F,I; 500 μm in G,J; 500 μm in H,K; 100 μm in L-O.

anterior portion of the brain without crossing the midline (Fig. 1O, arrowheads). Thus, *Smed-roboA* is required for the proper guidance of visual axons during regeneration.

Ectopic pharyngeal development and cephalic outgrowth after *Smed-roboA* RNAi

Unexpectedly, after *Smed-roboA* RNAi, approximately 67% (34/51) of anterior regenerates also produced a supernumerary pharynx between the pre-existing pharynx and the newly regenerated head. The ectopic pharynx typically formed lateral to the midline and closer to the position of the ventral nerve cord (VNC). The extent of ectopic pharyngeal development varied from small masses of pharyngeal cells to a morphologically distinguishable, complete pharynx (Fig. 2A,B; magenta asterisks, ectopic pharynges). Ectopic pharyngeal cells were detected in the pre-pharyngeal region by in situ hybridization using a pharynx-specific *laminin* (Fig. 2D, magenta asterisk); expression of this marker was restricted to the pharynx in controls (Fig. 2C, white asterisk).

Ectopic pharynges (Fig. 2A,B, magenta asterisks) developed with reversed anteroposterior polarity, as revealed by the opening of the pharyngeal lumen (Fig. 2A, magenta arrow) towards the anterior of the animal. This alteration of polarity could also be observed in the gut. In triclad planarians, the digestive system consists of three main gut branches connected to the central pharynx: one branch grows anteriorly along the midline, ending at the level of the photoreceptors; the other two branches grow posteriorly, lateral to the pharynx and dorsal to the ventral nerve cords, extending through the tail. In three *Smed-roboA* RNAi animals, two gut branches developed lateral to the ectopic pharynx (Fig. 2B), as they would in post-pharyngeal regions. The ectopic gut branches were connected to the main digestive tract of the animal (Fig. 2B, arrows). None of the animals developed an ectopic mouth opening (the planarian pharynx protrudes through the mouth to ingest food), so it is unlikely that the ectopic pharynges were functional.

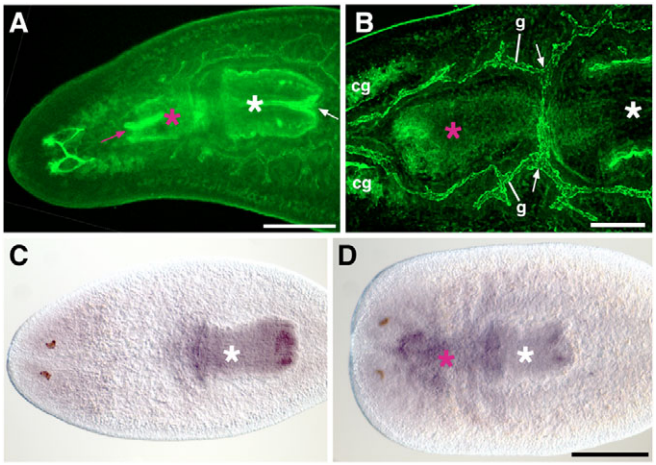

Fig. 2. Supernumerary pharynx formation after *Smed-roboA* RNAi. (**A**,**B**) Confocal projections showing ectopic pharynges after 16 days of regeneration and two rounds of RNAi treatment. Anti-phosphotyrosine and anti-VC-1 labeling is shown. In A, arrows indicate pharyngeal opening; in B, arrows indicate connections between ectopic and pre-existing gut. (**C**,**D**) *laminin* (DN293829) in situ hybridization in 16-day regenerates. (C) Control; (D) *Smed-roboA* RNAi. In all panels, white asterisks indicate original pharynges; magenta asterisks show ectopic pharynges. Anterior is to the left. cg, cephalic ganglia; g, ectopic gut branches. Scale bars: 200 μm in A; 100 μm in B; 300 μm in C,D.

Furthermore, approximately 13% (9/67) of *Smed-roboA* RNAi anterior regenerates produced an ectopic, dorsal outgrowth between the newly regenerated cephalic region and the pre-existing pharynx (Fig. 3A-E). All samples that produced an ectopic outgrowth also developed an ectopic pharynx. These outgrowths were first visible as small, unpigmented regions within the uninjured tissues close to the wound; they became more evident after 2 weeks of regeneration (Fig. 3A, arrowhead). In 7/9 cases, these outgrowths appeared lateral to the midline (Fig. 3B). The cephalic identity of these outgrowths was demonstrated both morphologically and by using molecular markers for various head-specific cell types: photosensitive cells (Fig. 3C), pigment cups of the photoreceptors (Fig. 3D, arrow), sensory cells (Fig. 3D, purple labeling) and brain-specific cells (Fig. 3E) differentiated within these outgrowths. Even in the absence of

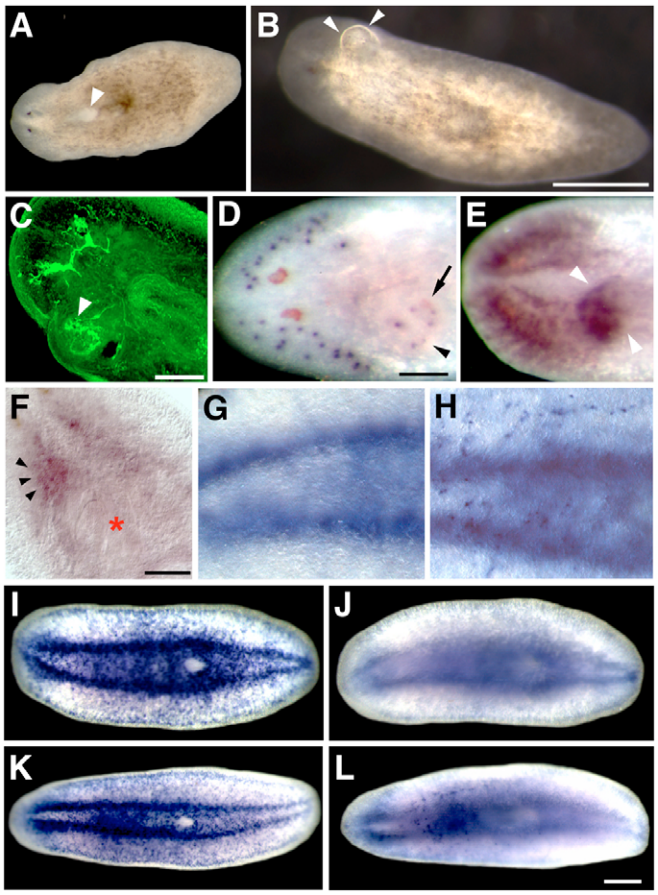

Fig. 3. Development of ectopic cephalic outgrowths after *Smed-roboA* RNAi. Living planarians imaged at 16 days (**A**) and 33 days (**B**) after amputation. (**C-E**) Cephalic neural markers in outgrowths. (C) Visual-cell marker, VC-1; confocal projection at 35 days after amputation. (D) Sensory-cell marker, *cintillo* (Oviedo et al., 2003); arrow indicates photoreceptor pigment cells. (E) Clone H.10.2f, marker of cephalic ganglia. (D,E) At 16 days after amputation. In A-E, arrowheads indicate ectopic outgrowths. (**F**) Ectopic *Smed-netrin1* expression (arrowheads) near an ectopic pharynx (red asterisk); 18-day regenerate. (**G-L**) Expression of the ventral marker *anosmin-1* (AY066061) in an 18-day regenerate. (G) Control: *anosmin-1*-positive cells are not observed in dorsal views. (H) *Smed-roboA* RNAi: *anosmin-1*-positive cells are detected dorsally. (I-L) Control (I,J) and *Smed-roboA* RNAi (K,L) planarians viewed ventrally (I,K) and dorsally (J,L). Anterior to the left. Scale bars: 1.5 mm in A (bar shown in B); 1 mm in B; 100 μm in C-E; 100 μm in F; 500 μm in I-L.

obvious outgrowths, ectopic *Smed-netrin1*-expressing cells were detected (Fig. 3F, arrowheads); these cells are normally confined to two narrow rows along the medial cephalic ganglia and ventral nerve cords (Cebrià and Newmark, 2005). In addition, a ventral-specific marker was detected dorsally (Fig. 3G,H). A gene similar to *anosmin-1*, implicated in Kallman's syndrome in humans (Franco et al., 1991; Legouis et al., 1991), is expressed both in a subset of cells of the CNS and ventrally, in cells beneath the ventral musculature (Fig. 3I; data not shown). No *anosmin-1*-positive cells were detected in dorsal views of control planarians (Fig. 3G,J). However, in 8 out of 14 *Smed-roboA* RNAi animals, ectopic *anosmin-1*-expressing cells were detected dorsally (Fig. 3H), confined to the region between the newly regenerated head and the pharynx (Fig. 3L). Using a clone with weak similarity to *septin* (DN302617) as a marker for dorsal mesenchymal cells, we did not observe a concomitant displacement of these cells ventrally (data not shown). Thus, it appears that the polarity of the tissues in which ectopic structures form is only partially altered.

Disruption of neuronal connectivity following *Smed-roboA* RNAi

Because of the conserved role of robo genes in nervous system development, we examined the pattern of the regenerated CNS in *Smed-roboA* RNAi animals. Detailed examination revealed defects in the regeneration of the cephalic ganglia. The anterior commissure connecting the two ganglia was greatly reduced (Fig. 4B, 37/51; compare with control in 4A); in extreme cases, no commissure was observed between the two lobes (see Fig. 1O, arrow; 10/51). In wild-type animals, the amputated VNCs grew into the blastema beneath the newly regenerated cephalic ganglia. Both structures overlapped after the completion of regeneration, with the cephalic ganglia positioned directly above the underlying VNCs (Fig. 4C,E,G,I) (Okamoto et al., 2005). By contrast, after *Smed-roboA* RNAi, the regenerated cephalic ganglia were mis-positioned relative to the nerve cords (Fig. 4D,F,H,J). The ganglia were displaced laterally, resulting in a curvature in the VNCs as they reconnected to the regenerated ganglia (Fig. 4F). In the majority of *Smed-roboA* RNAi knockdown animals (29/51; 57%), a more dramatic dissociation between the regenerated cephalic ganglia and VNCs was observed (Fig. 4H,J). In these cases, the newly regenerated cephalic ganglia regenerated lateral to the VNCs; the VNCs appeared truncated and failed to extend to the anterior-most portion of the brain. These defects were observed as early as day 5 of regeneration (Fig. 4H), well before the appearance of ectopic structures. Despite these defects in the organization of the regenerated CNS, no obvious behavioral defects were observed.

An ectopic pharynx was observed in approximately 90% (26/29) of the *Smed-roboA* RNAi animals that showed a clear disconnection between the brain and the VNCs. By contrast, an ectopic pharynx was observed in only 36% (8/22) of the knockdown animals in which these misconnections were not apparent with the markers that we used. Posterior regeneration (head pieces regenerating new pharynx and posterior regions) proceeded normally in *Smed-roboA* RNAi knockdown animals: the VNCs grew properly into the new posterior regions and no ectopic pharynges or outgrowths developed (data not shown).

The above results suggest that the nervous system may play an important role in patterning the newly formed anterior tissues during planarian regeneration. Following *Smed-roboA* RNAi, the VNCs and the newly formed cephalic ganglia are not connected properly. Almost all of the planarians with these neural defects produced ectopic pharynges and cephalic outgrowths. The CNS-specific expression of *Smed-roboA* during regeneration (Fig. 1C-E) and the observation that the improper connection of the VNCs and ganglia preceded ectopic tissue growth (Fig. 4H) suggest that the development of ectopic structures results from primary defects in the regenerated nervous system. A recent high-throughput RNAi screen in planarians reported that the knockdown of clone H.68.4a, which has low similarity to slit genes, resulted in the development of

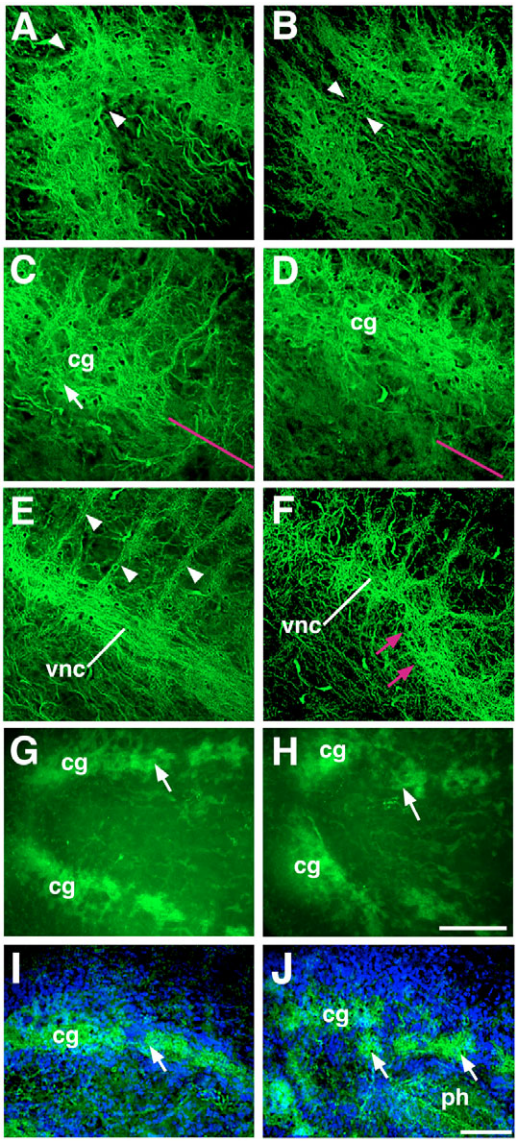

Fig. 4. Defects in CNS regeneration after *Smed-roboA* RNAi. (**A-F**) Anti-tubulin immunofluorescence in control (A,C,E) and *Smed-roboA* RNAi (B,D,F) 16-day regenerates. Arrowheads in A and B delimit the anterior commissure. (C,D) Regenerated cephalic ganglia in control (C) and *Smed-roboA* RNAi (D) planarians; magenta lines mark the position of the VNCs in more-ventral sections (shown in E and F). (E) Control: normally regenerated VNC; arrowheads show regularly spaced lateral processes. (F) *Smed-roboA* RNAi: improperly regenerated VNC; lateral processes are disorganized; magenta arrows indicate curvature. (**G-J**) Anti-phosphotyrosine immunofluorescence (green) in 5-day (G,H) and 16-day (I,J) regenerates. Hoechst staining is shown in blue. (G,I) Controls: regenerated cephalic ganglia overlap the regenerated nerve cord (arrows). (H,J) *Smed-roboA* RNAi: regenerated cephalic ganglia are not connected properly to the truncated nerve cord (arrows). (A-F) Anterior to the top left. (G-J) Anterior to the left. Images are confocal projections. Scale bars: 100 μm. cg, cephalic ganglia; vnc, ventral nerve cords; ph, pharynx.

ventral cephalic outgrowths (Reddien et al., 2005). Further analyses should clarify the extent of similarities between the defects observed after H.68.4a and *Smed-roboA* RNAi, and whether or not these two genes could encode a ligand-receptor pair.

In planarians, ectopic outgrowths have also been observed following grafts in which dorsal and ventral tissues are juxtaposed (Santos, 1931; Kato et al., 1999). Likewise, the juxtaposition of anterior and posterior tissues leads to the development of ectopic pharynges (Kobayashi et al., 1999). Thus, discontinuities in anteroposterior or dorsoventral positional values can lead to changes in cell proliferation (resulting in tissue outgrowth) and differentiation (producing new tissues and organs). We suggest that the improper connection between the cephalic ganglia and ventral nerve cords in *Smed-roboA*-knockdown animals mimics the effects of transplantation or amputation, in which the cephalic ganglia and VNCs are separated. In the absence of this connection, we infer that neurally derived signals are sent to the surrounding tissues; these signals could alter positional identities and trigger the production of an ectopic pharynx and a cephalic outgrowth. This idea is consistent with previous observations showing an increase of neurosecretory granules following amputation (Sauzin-Monnot, 1972) and the stimulation of mitogenic activity in planarians by substance P and substance K (Baguñà et al., 1989).

Such a role for the planarian nervous system may reflect an evolutionarily conserved function in pattern formation during regeneration; thus, in annelids, deflected cut ends of anteriorly facing nerve cords can give rise to ectopic heads, whereas deflected cut ends of posteriorly facing nerve cords induce the differentiation of ectopic tails (Kiortsis and Moraitou, 1965). In urodele amphibians, the dependence of limb regeneration on the nervous system has been clearly shown (Singer and Craven, 1948; Singer, 1952); deviation of the caudal spinal cord can induce supernumerary tails (Kiortsis and Droin, 1961) and nerve deviation to a skin wound can induce ectopic limbs (Egar, 1988; Endo et al., 2004). Further analyses, combining the tools of functional genomics now available for studying planarians (Newmark and Sánchez Alvarado, 2002; Reddien et al., 2005), will help us to identify the signals that serve to re-establish proper pattern during planarian regeneration.

We would like to thank Gene Robinson, Huey Hing, Dave Forsthoefel, Ricardo Zayas and Tingxia Guo for helpful comments on the manuscript; Alejandro Sánchez Alvarado for providing asexual EST clones; and Kiyokazu Agata for providing VC-1. Planarian genomic-sequence data were generated by the Washington University Genome Sequencing Center in St Louis. F.C. was supported by a Long-Term Fellowship from EMBO and the programme Beatriu de Pinós of Generalitat de Catalunya; he thanks Emili Saló for support. This work was supported by NIH grant R01 HD43403 and NSF CAREER Award IBN-0237825 to P.A.N. P.A.N. was a Damon Runyon Scholar supported by the Damon Runyon Cancer Research Foundation (DRS 33-03).

Supplementary material

Supplementary material for this article is available at
http://dev.biologists.org/cgi/content/full/134/5/833/DC1

References

Agata, K. (2003). Regeneration and gene regulation in planarians. *Curr. Opin. Genet. Dev.* **13**, 492-496.
Araujo, S. J. and Tear, G. (2003). Axon guidance mechanisms and molecules: lessons from invertebrates. *Nat. Rev. Neurosci.* **4**, 910-922.
Baguñà, J., Saló, E. and Romero, R. (1989). Effects of activators and antagonists of the neuropeptides substance P and substance K on cell proliferation in planarians. *Int. J. Dev. Biol.* **33**, 261-266.
Brose, K., Bland, K. S., Wang, K. H., Arnott, D., Henzel, W., Goodman, C. S., Tessier-Lavigne, M. and Kidd, T. (1999). Slit proteins bind Robo receptors and have an evolutionarily conserved role in repulsive axon guidance. *Cell* **96**, 795-806.
Cebrià, F. and Newmark, P. A. (2005). Planarian homologs of netrin and netrin receptor are required for proper regeneration of the central nervous system and the maintenance of nervous system architecture. *Development* **132**, 3691-3703.
Cebrià, F., Nakazawa, M., Mineta, K., Ikeo, K., Gojobori, T. and Agata, K. (2002). Dissecting planarian central nervous system regeneration by the expression of neural-specific genes. *Dev. Growth Differ.* **44**, 135-146.
Chandebois, R. (1980). The dynamics of wound closure and its role in the programming of planarian regeneration. II–Distalization. *Dev. Growth Differ.* **22**, 693-704.
Egar, M. W. (1988). Accessory limb production by nerve-induced cell proliferation. *Anat. Rec.* **221**, 550-564.
Endo, T., Bryant, S. V. and Gardiner, D. M. (2004). A stepwise model system for limb regeneration. *Dev. Biol.* **270**, 135-145.
Franco, B., Guioli, S., Pragliola, A., Incerti, B., Bardoni, B., Tolonrenzi, R., Carrozzo, R., Maestrini, E., Pieretti, M., Taillon-Miler, P. et al. (1991). A gene deleted in Kallmann's syndrome shares homology with neural cell adhesion and axonal path-finding molecules. *Nature* **353**, 529-536.
Inatani, M. (2005). Molecular mechanisms of optic axon guidance. *Naturwissenschaften* **92**, 549-561.
Kato, K., Orii, H., Watanabe, K. and Agata, K. (1999). The role of dorsoventral interaction in the onset of planarian regeneration. *Development* **126**, 1031-1040.
Kato, K., Orii, H., Watanabe, K. and Agata, K. (2001). Dorsal and ventral positional cues required for the onset of planarian regeneration may reside in differentiated cells. *Dev. Biol.* **233**, 109-121.
Kidd, T., Bland, K. S. and Goodman, C. S. (1999). Slit is the midline repellent for the Robo receptor in Drosophila. *Cell* **96**, 785-794.
Kiortsis, V. and Droin, A. (1961). Caudal regeneration in Urodela (induction and reactivity of the region). *J. Embryol. Exp. Morphol.* **9**, 77-96.
Kiortsis, V. and Moraitou, M. (1965). Factors of regeneration in Spirographis spallanzanii. In *Regeneration in Animals and Related Problems* (ed. V. Kiortsis and H. A. L. Trampusch), pp. 250-261. Amsterdam: North Holland.
Kobayashi, C., Nogi, T., Watanabe, K. and Agata, K. (1999). Ectopic pharynxes arise by regional reorganization after anterior/posterior chimera in planarians. *Mech. Dev.* **89**, 25-34.
Legouis, R., Hardelin, J. P., Levilliers, J., Claverie, J. M., Compain, S., Wunderle, V., Millasseau, P., Le Paslier, D., Cohen, D., Caterina, D. et al. (1991). The candidate gene for the X-linked Kallmann syndrome encodes a protein related to adhesion molecules. *Cell* **67**, 423-435.
Newmark, P. A. and Sánchez Alvarado, A. (2002). Not your father's planarian: a classic model enters the era of functional genomics. *Nat. Rev. Genet.* **3**, 210-219.
Nogi, T. and Levin, M. (2005). Characterization of innexin gene expression and functional roles of Gap-junctional communication in planarian regeneration. *Dev. Biol.* **287**, 314-335.
Okamoto, K., Takeuchi, K. and Agata, K. (2005). Neural projections in planarian brain revealed by fluorescent dye tracing. *Zool. Sci.* **22**, 535-546.
Oviedo, N., Newmark, P. A. and Sánchez Alvarado, A. (2003). Allometric scaling and proportion regulation in the freshwater planarian *Schmidtea mediterranea*. *Dev. Dyn.* **226**, 326-333.
Reddien, P. W. and Sánchez Alvarado, A. (2004). Fundamentals of planarian regeneration. *Annu. Rev. Cell Dev. Biol.* **20**, 725-757.
Reddien, P. W., Bermange, A. L., Murfitt, K. J., Jennings, J. R. and Sanchez Alvarado, A. (2005). Identification of genes needed for regeneration, stem cell function, and tissue homeostasis by systematic gene perturbation in planaria. *Dev. Cell* **8**, 635-649.
Saló, E. and Baguñà, J. (1985). Proximal and distal transformation during intercalary regeneration in the planarian *Dugesia (S) mediterranea*. *Rouxs Arch. Dev. Biol.* **194**, 364-368.
Sánchez Alvarado, A. and Newmark, P. A. (1999). Double-stranded RNA specifically disrupts gene expression during planarian regeneration. *Proc. Natl. Acad. Sci. USA* **96**, 5049-5054.
Sánchez Alvarado, A., Newmark, P. A., Robb, S. and Juste, R. (2002). The *Schmidtea mediterranea* database as a molecular resource for studying platyhelminthes, stem cells, and regeneration. *Development* **129**, 5659-5665.
Santos, F. V. (1931). Studies on transplantation in planaria. *Physiol. Zool.* **4**, 111-164.
Sauzin-Monnot, M. J. (1972). Étude ultrastructurale du tissu nerveux et des produits de sécrétion nerveuse, au cours des premières heures de régénération de la planaire *Polycelis nigra* (Turbellarié- Triclade) au niveau de la blessure. *Ann. Embryol. Morphogen.* **5**, 257-265.
Singer, M. (1952). The influence of the nerve in regeneration of the amphibian extremity. *Q. Rev. Biol.* **27**, 169-200.
Singer, M. and Craven, L. (1948). The growth and morphogenesis of the regenerating forelimb of adult *Triturus* following denervation at various stages of development. *J. Exp. Zool.* **108**, 279-308.
Umesono, Y., Watanabe, K. and Agata, K. (1999). Distinct structural domains in the planarian brain defined by the expression of evolutionarily conserved homeobox genes. *Dev. Genes Evol.* **209**, 31-39.
Zayas, R. M., Hernandez, A., Habermann, B., Wang, Y., Stary, J. M. and Newmark, P. A. (2005). The planarian *Schmidtea mediterranea* as a model for epigenetic germ cell specification: analysis of ESTs from the hermaphroditic strain. *Proc. Natl. Acad. Sci. USA* **102**, 18491-18496.

Table S1. Summary of the phenotypes observed after *Smed-roboA* RNAi

Visual system

	Normal	Ectopic loops	No optic chiasm	Other[a]
Control	38	1	0	4
Smed robo1 RNAi	3	33	8[b]	3

Regenerated CNS

Brain anterior commissure:	~Normal	Thin	Absent
	4/51	37/51	10/51

Brain/VNC relationship:	Disconnected	Lateral
	29/51	22/51

Frequency of ectopic pharynx development in animals with CNS-regeneration defects

	Brain/VNC disconnected	Brain lateral to VNC
Ectopic pharynx	26/29	8/22

Frequency of ectopic pharynx and cephalic outgrowth development in animals with ectopic loops in the visual system

	Ectopic pharynx	Outgrowths
	22/39	4/39

[a]Abnormal phenotypes different from those described in text.
[b]6/8 also showed ectopic loops.